

Adsorption of diazinon using Cd-MOF nanoparticles before determination by UV-Vis spectrometer: isotherm, kinetic and thermodynamic study

Faeze Khakbaz^a, Mohamad Mahani^{b*} and Mehdi Yoosefian^b

^a Department of Chemistry, Shahid Bahonar University, Kerman, Iran

^b Department of Chemistry, Faculty of Chemistry and Chemical Engineering, Graduate University of Advanced Technology, Kerman, 7631818356, Iran.

ARTICLE INFO:

Received 15 Feb 2022

Revised form 20 Apr 2022

Accepted 25 May 2022

Available online 29 Jun 2022

Keywords:

Cadmium Metal–Organic Frameworks,
Diazinon,
UV-Vis spectrometer,
Adsorption kinetic,
Adsorption thermodynamic,
Pesticides

ABSTRACT

In this work, cadmium metal–organic frameworks (Cd-MOF) has been prepared using a hydrothermal method and characterized by the SEM, elemental mapping, XRD, EDS, and BET analysis. The diazinon stability has been investigated in various pH (4-8) and temperature (298°K – 323°K) using UV-Vis spectrometer in the range of 230 – 280 nm, at its main absorption peak at 247 nm. Adsorption behaviors of diazinon on the Cd MOF were considered in different conditions. UV-Vis spectroscopy was used to monitor the removal of diazinon using the Cd MOF. The adsorption capacity of 138 mg g⁻¹ was obtained. The effect of temperature (298°K -323°K), pH (4-8), adsorbent dose (1-7 mg), initial concentration (4-12 mg L⁻¹), stirring speed (0-500 rpm), and adsorption kinetics were studied using batch rout. All the studied parameters have shown significant effects on the efficiency of removal of diazinon by the Cd MOF. The adsorption thermodynamic was investigated in the temperature range of 298°K to 323°K and it has shown the endothermic nature of adsorption of diazinon using prepared Cd MOF. The adsorption isotherm follows by the Langmuir isotherm model. It was demonstrated that synthesized adsorbent could be effectively used for the removal of diazinon from water.

1. Introduction

The use of pesticides in agriculture to control unwanted insects and disease carriers increases food production. Widespread use of pesticides in agriculture and public health programs endangers public health with issues such as acute human poisoning and environmental pollution [1]. According to the World Health Organization (WHO), the number of acute pesticide poisonings in developing countries is increasing every year. In 1982, it was estimated that while

developing countries accounted for only 15% of global pesticide use, more than 50% of pesticide poisoning occurred in those countries due to misuse [2]. Organophosphates, phosphorus-containing compounds which are derived from phosphoric acid, are generally used as insecticides among pesticides and are usually the most toxic insecticides to vertebrates. Residual amounts of organophosphates pesticides have been identified in cereals, vegetables, water bodies, soil, water, and other agricultural products [3]. Due to the widespread use of pesticides, their toxic effects have been observed in humans [4]. The mechanism of action is based on the inhibition of acetylcholinesterase activity by

*Corresponding Author: [Mohamad Mahani](mailto:mohamad.mahani@shbu.ac.ir)

Email: mohmahani@gmail.com

<https://doi.org/10.24200/amecj.v5.i02.175>

covalently binding to its serine residues, thereby stopping nerve impulses that lead to death [5]. The lipophilic nature of organophosphates, facilitates their interaction with the cell membrane and led to disrupts the bilayer structure of phospholipids in visceral organs [6]. Acute poisoning by organophosphates stimulates muscarinic receptors, and diarrhea, abdominal pain, sweating, excessive salivation, and other symptoms are appeared [7]. In addition, stimulation of nicotine receptors in skeletal muscle neuromuscular connections by organophosphates cause weakness, involuntary contraction, and paralysis [8]. These pesticides have many adverse effects on the reproductive system, urinary system and human immune system [9]. Among the most commonly used organophosphates pesticides, O,O-Diethyl O- [4-methyl-6- (propane2-yl)pyrimidin-2-yl]phosphorothioate, INN - Dimpylate (diazinon) is a synthetic chemical that is used worldwide in agriculture to control insects in crops, vegetables, fruits, grass, and ornamental plants [11]. Diazinon is classified as a moderately dangerous organophosphate class II insecticide and can be absorbed through the gastrointestinal tract, skin, or respiratory tract upon inhalation [12]. Diazinon also leads to hyperglycemia, and depletion of glycogen from the brain and peripheral tissues along with increased glycogen phosphorylase activity in the brain and liver [13]. Recently, the removal of diazinon from water using adsorption methods has attracted much attention. For determining percentages of removal various methods such as simulation, spectroscopy, and chromatography have been used [14, 15]. Various materials such as multi-walled carbon nanotubes [16], activated carbon [17], bismuth oxide-fullerene nanoparticles [18], mesoporous silica [19] and, metal-organic frameworks [20] and other porous materials [21] have been used as adsorbents. Metal-organic framework, which is composed of metal ions or clusters of organic linkers, are crystalline materials

that have a variety of applications in the removal of contaminants [22] drug delivery [23], catalysis [24] separation [19], electronic devices [25] gas storage [26], and sensors [27]. Due to the adjustable porosity, high surface area, adsorptive properties, and variety of structures MOFs are effective agents for the removal of pesticides from water. MOFs are synthesized using many methods such as ionothermal [28], solvent evaporation [29], self-assembly of primary building blocks [30], mechanochemical [31], electrochemical [32], ultrasonic [33], microwave [34], solvothermal [35] and hydrothermal [20, 36] methods.

In this work, Cd MOF was prepared using a hydrothermal route. The synthesized porous nanomaterial was used for the removal of diazinon from water. The temperature, pH, contact time, amount of adsorbent, stirring speed effect, adsorption isotherms, and adsorption kinetics were investigated.

2. Experimental

2.1. Materials and apparatus

Cadmium (II) nitrate tetrahydrate (CAS N.: 10022-68-1; Sigma, Germany), fumaric acid (CAS N.: 110-17-8; Sigma, Germany), and diazinon (CAS N.: 333-41-5; Merck, Germany) were used without any purification. The chemical structure of diazinon is shown in Figure 1. The sample pH was adjusted with hydrochloric acid (CAS N.: 7647-01-0; Merck, Germany) and sodium hydroxide (CAS N.: 1310-73-2; Merck, Germany). The absorption spectra were obtained by using an Agilent Cary 50 UV-Vis spectrometer, with 1.0 cm quartz cells. The crystal structure of Cd MOF was analyzed by Bruker Advance-D8 equipped with Cu K α radiation (Bruker, Germany). The morphology was obtained by an S-4800 HITACHI scanning electron microscope at 10 kV, 100 mA (Hitachi, Japan). The pore volume and surface area of the Cd MOF were determined by BET method using Sorptomatic 1990 after degassing at 150°C (Thermo Fisher Scientific, USA.)

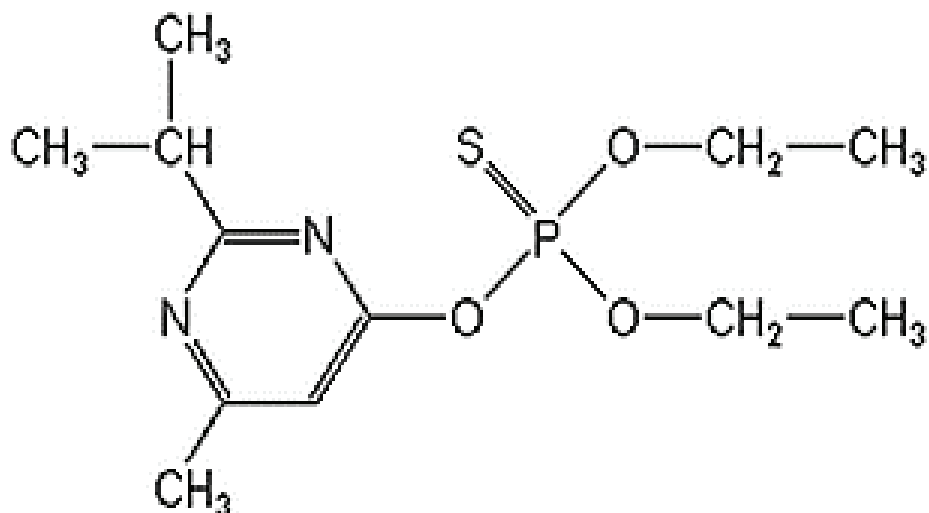
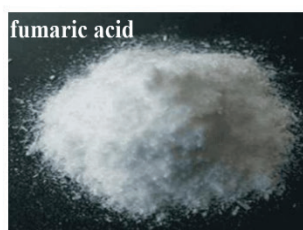
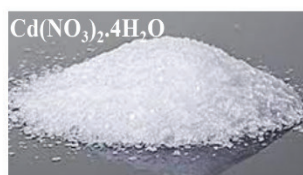


Fig.1. Chemical structure of diazinon

2.2. Synthesis of the Cd-MOF

Cd MOF was synthesized according to the previous reports with minor modifications [20]. 8.9 g $\text{Cd}(\text{NO}_3)_2 \cdot 4\text{H}_2\text{O}$, 5.22 g fumaric acid, and 3.6 g NaOH were dispersed in 50 mL ultrapure water and were stirred for 30 minutes. The solution was

transferred into a 100 ml Teflon-lined hydrothermal reactor and incubated in 180°C for 48 h (Scheme 1). The autoclave was cooled to room temperature for 12 h. The product was centrifuged at 10000 g for 15 minutes, washed several times with distilled water, and dried at 50°C overnight.



Scheme 1. Synthesis of Cd MOF

2.3. Adsorption study procedure

Removal studies of diazinon by the Cd MOF were carried out in the batch procedure. UV-Vis spectroscopy was used to monitor equilibrium concentrations of diazinon. The calibration curve was plotted for different concentrations of diazinon and their corresponding absorbance at 248 nm. After the removal process, the residual concentration of diazinon was deducted from the calibration curve. The uptake capacity and removal efficiency were determined by comparing the concentration of diazinon before and after adsorption, according to the following equation 1 and 2:

$$\text{Removal efficiency (\%)} = (C_i - C_e) / C_i \times 100 \quad (\text{Eq. 1})$$

$$\text{Uptake capacity } Q_e \text{ (mg g}^{-1}\text{)} = (C_i - C_e) \times V/m \quad (\text{Eq. 2})$$

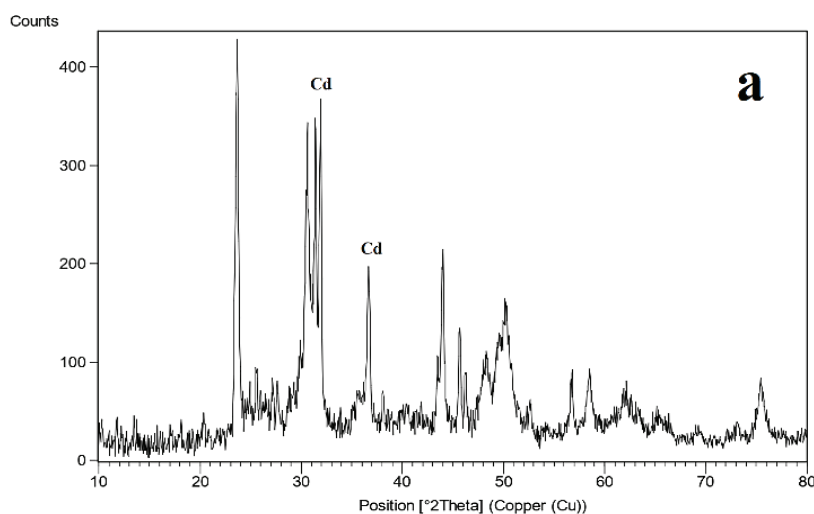
Q_e is the amount of diazinon adsorbed on the surface of MOF. Where C_i and C_e are the initial and equilibrium concentration of diazinon solution, V is the volume of diazinon solution, and m is the weight of MOF. In the batch procedure, the influence of effective parameters such as contact time, adsorbent dose, initial concentration of insecticides, temperature, pH, and the stirring speed was investigated.

3. Results and discussion

3.1. characterization of Cd MOF

Figure 2a shows the XRD pattern of the synthesized Cd MOF. The pattern exhibited diffraction peaks that were similar to the plan of Cd (No. 01-085-0989). The crystal size of the Cd MOF was calculated using the Debye-Scherrer equation at about 21 nm.

The morphology of Cd MOF was characterized by SEM, which is shown in Figure 2b. The obtained SEM images show that the prepared Cd MOF are cubic and have uniform size distributions. The energy-dispersive X-ray spectroscopy (EDS) has been used to characterize the chemical composition of synthesized nanocrystals. Figure 2c and 2d show the chemical elemental mapping and EDS of the Cd MOF. The EDS results are revealed that the synthesized nanocrystals have composed of Cd, O, and C. In addition, the elemental mapping shows that the elements are homogeneously distributed through the MOFs. The specific surface area of the prepared Cd MOFs is explained using Brunaur-Emmett-Teller (BET) method. The mean pore diameter, surface area, and total pore volume of the nanocrystals were calculated at about 15.5 nm, $0.4 \text{ m}^2 \text{ g}^{-1}$, and $0.0014 \text{ cm}^3 \text{ g}^{-1}$, respectively.



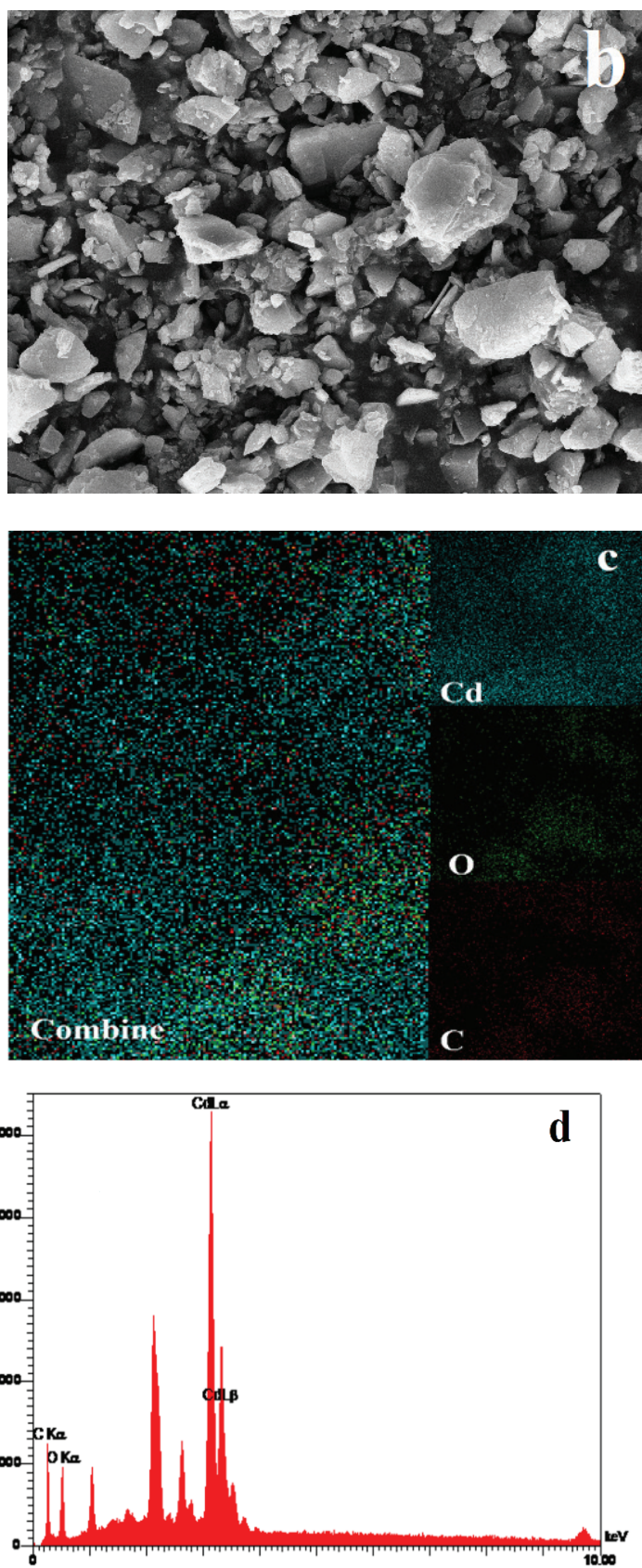


Fig. 2. Characterization of Cd MOF, a) The XRD pattern, b) The SEM image, c) The elemental mapping, and d) The EDS analysis of Cd MOF

3.2. Adsorption of diazinon onto Cd MOF

3.2.1. Optical stability of diazinon

Diazinon stability was studied in various pH and temperature conditions. As shown in Figure 3, temperature and pH changes of the diazinon solution don't have significant effects on the absorption intensity at 248 nm. Therefore, it can be said that diazinon is stable at the studied temperature and pH values.

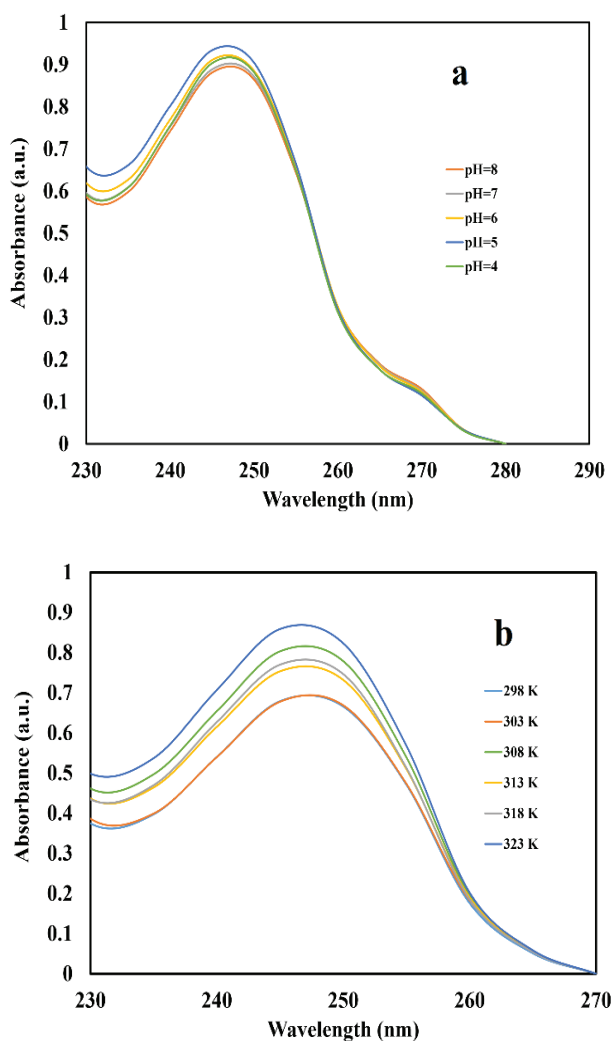


Fig. 3. Effect of various (a) pH and (b) temperature on diazinon absorption spectra

3.2.2. Effect of adsorbent dose

For investigation the optimized mass of Cd MOF in adsorption process, various amounts (1-7 mg) of adsorbent were added to the constant volume (30 ml) of 12-ppm diazinon solution under the same

conditions and stirred at 300 rpm. The absorption spectra of solutions were recorded at a specific time. Figure 4 shows the removal efficacy and uptake capacity of different amounts of Cd MOF in various periods. It can be seen that the removal intensity of diazinon was increased from 37% to 95% with increasing the adsorbent dose from 1 to 7 mg at 15 minutes as the contact times. This increase is clearly due to the increase in surface area and adsorption sites. 3 mg of Cd MOF was chosen as the optimal amount of adsorbent for further experiments.

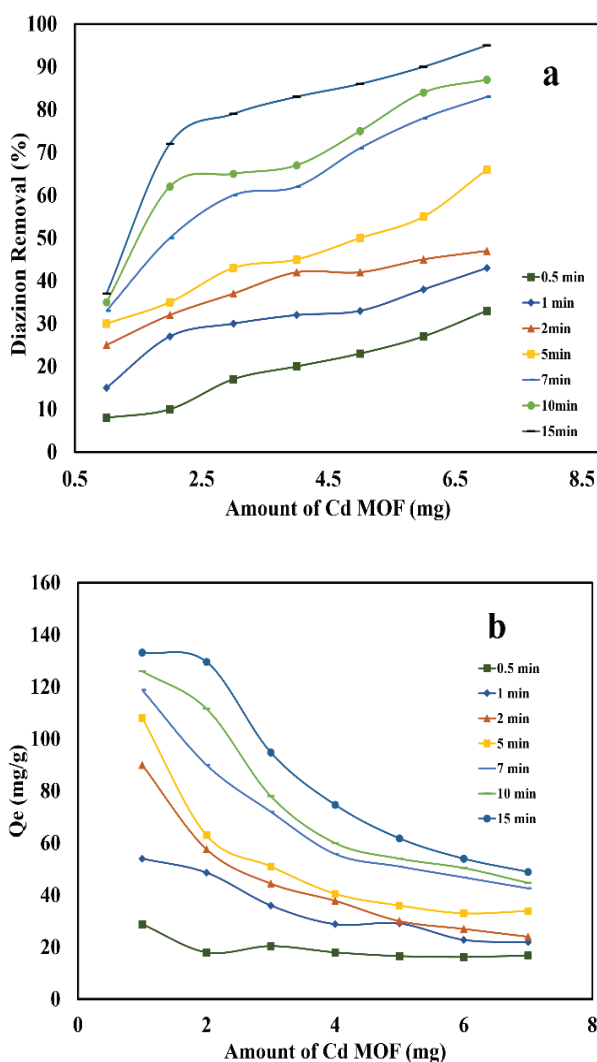


Fig. 4. Effect of adsorbent dose on (a) removal efficiency and (b) uptake capacity of Cd MOF (diazinon concentration = 12 ppm, natural pH, room temperature)

3.2.3. Effect of diazinon concentration

The plot of uptake capacities vs. initial diazinon concentrations in presence of 3 mg Cd MOF as the optimal amount of adsorbent and at various contact time were shown in Figure 5. It was shown that after 15 minutes, with increasing the initial diazinon concentration from 4 to 12 ppm, the uptake capacity increased from 42 To 95 mg g⁻¹. The increase of uptake capacity is probably due to increase in the mass gradient between the diazinon solution and Cd MOF with increasing the insecticide concentration.

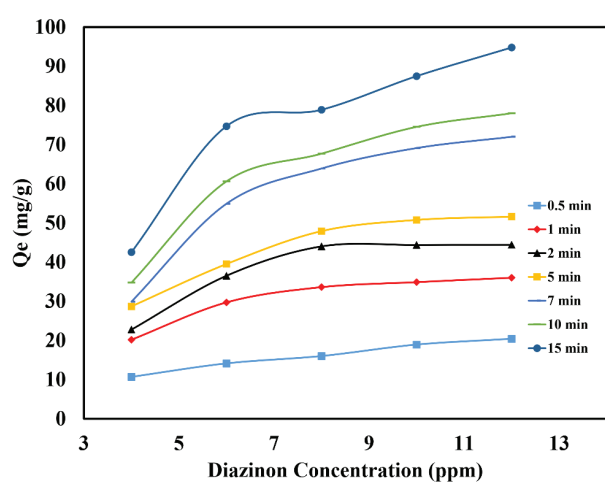


Fig. 5. Effect of initial diazinon concentration on uptake capacity of Cd MOF in various contact times (amount of adsorbent = 3 mg, natural pH, room temperature)

3.2.4. Effect of contact time

Figure 6 shows the plot of uptake capacity vs. contact time in presence of various amounts of Cd MOF (the diazinon concentration of 12 ppm), and different concentrations of diazinon (adsorbent dose of 3 mg) at natural pH and room temperature. According to the results, the diazinon is rapidly adsorbed and the optimal removal efficacy is obtained at 7 minutes. A large number of empty sites at the Cd MOF surface in the early minutes causes high adsorption efficacy. With time and occupied the active sites with diazinon molecules, the adsorption speed decreased impressively.

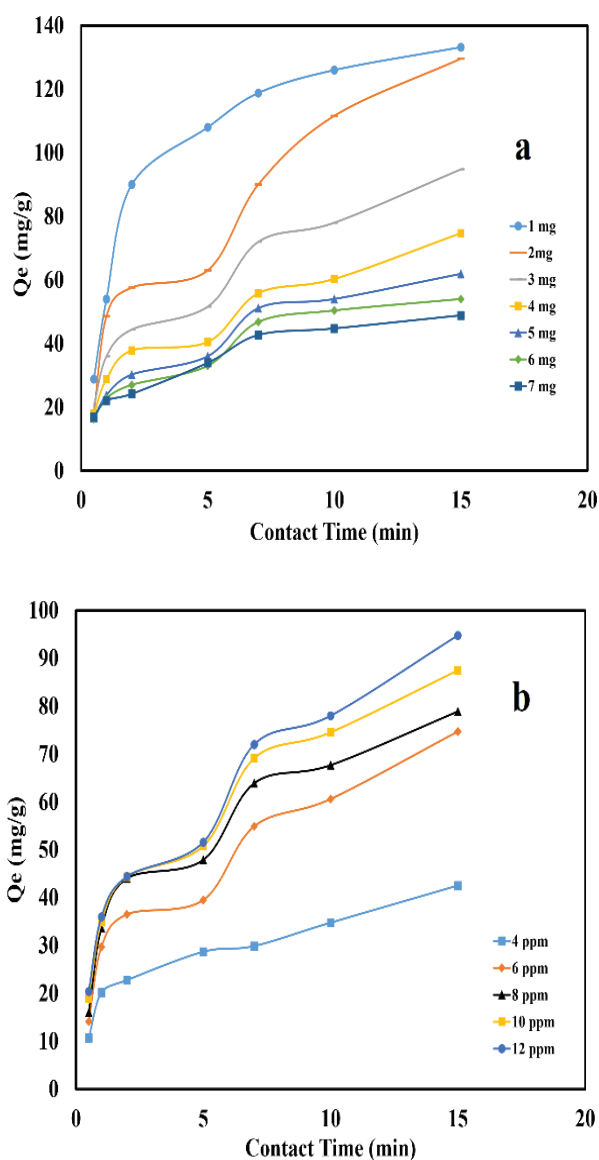


Fig. 6. Effect of contact time on uptake capacity of Cd MOF in (a) various amounts of adsorbent (diazinon concentration = 12 ppm, natural pH, and room temperature) (b) various concentrations of diazinon (amount of adsorbent = 3 mg, natural pH, and room temperature)

3.2.5. Effect of pH

The adsorption of diazinon onto Cd MOF was investigated in a pH range of 4-8 at room temperature. 3 mg of Cd MOF was added to 30 ml of 12 ppm diazinon solution and stirred at 300 rpm for 0.5 to 10 minutes. According to Figure 7, the removal efficiency of diazinon by Cd MOF was increased with an increase in pH. Figure

7b clearly shows increasing the uptake capacity from 43 to 58 mg g⁻¹ by increasing the pH from 4 to 8. The desirable removal at higher pH can be due to the cationic nature of diazinon. The presence of excess, H⁺ in acidic solution cause to decrease in the negative adsorbent site and it is not favored for positively charged diazinon ions. An increasing number of negative sites on the adsorbent can enhance the adsorption of diazinon at high pH.

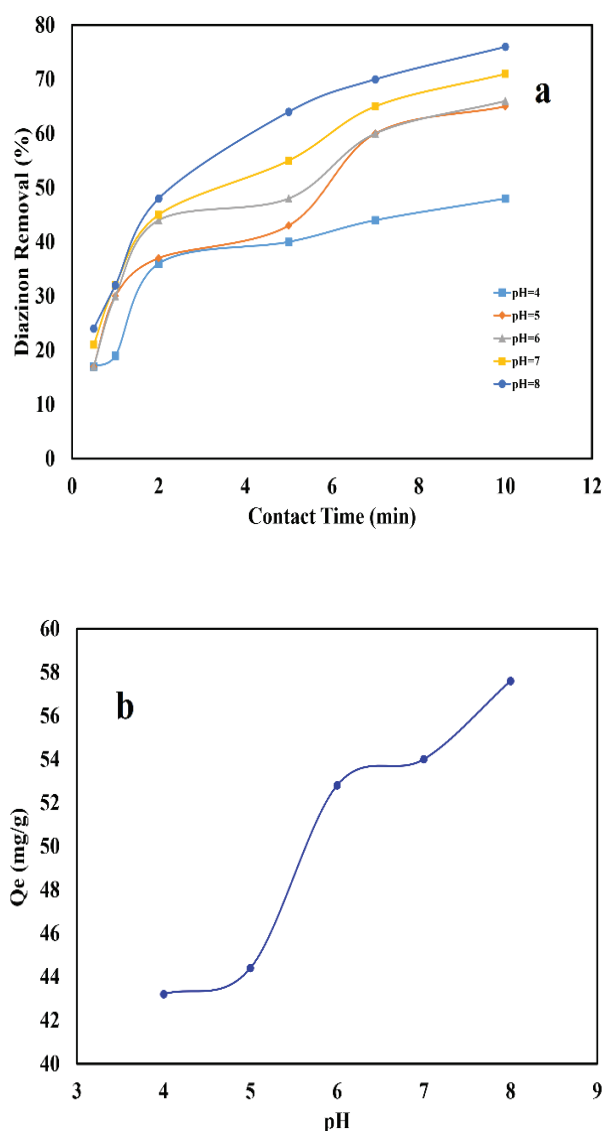


Fig. 7. Effect of pH on (a) removal efficiency of diazinon using Cd MOF at various contact times, (b) uptake capacity of Cd MOF at 7 minutes (diazinon concentration = 12 ppm, amount of adsorbent = 3 mg, and room temperature)

3.2.6. Effect of temperature

Removal of the diazinon was studied at various temperatures from 298 to 323 K in the presence of 3 mg of Cd MOF at different times. As shown in Figure 8, the adsorption efficiency has been increased with increasing in temperature. The increase of removal efficiency can be due to the endothermic nature of the adsorption process.

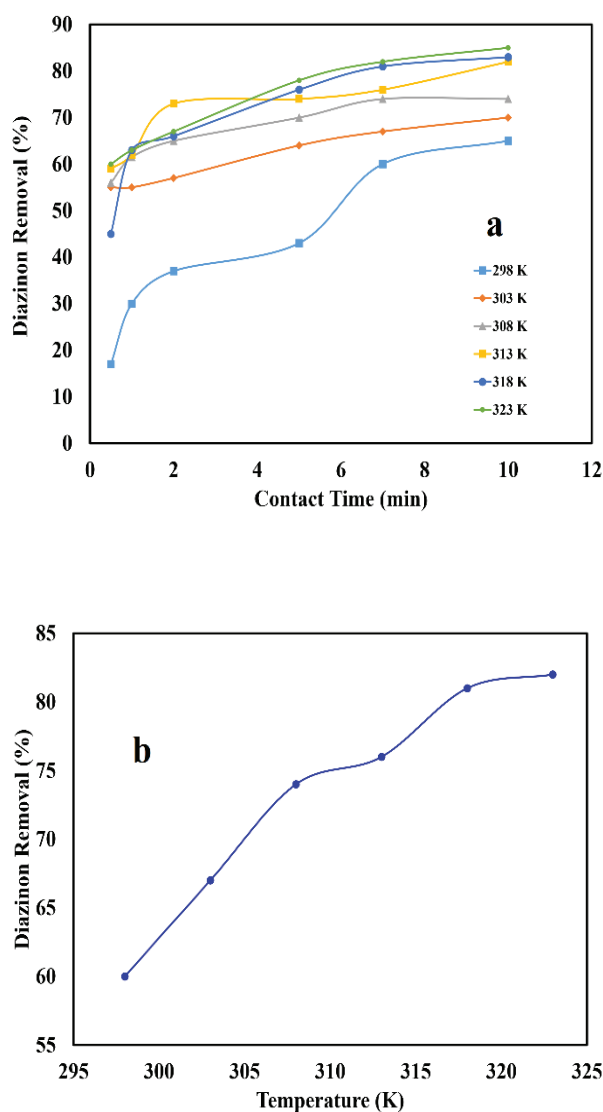


Fig. 8. Effect of temperature on removal efficiency of diazinon (a) at various times, (b) at 7 minutes as optimum time (dye concentration = 12 ppm, amount of adsorbent = 3 mg, and natural pH)

3.2.7. Effect of stirring speed

The effect of stirring speed on the removal of diazinon was studied at various stirring speeds (0 -

500 rpm) in identical conditions (natural pH, room temperature, 12 ppm initial diazinon concentration, 7 minutes as contact time). According to Figure 9, the stirring speed shows significant effect on removal rate in the removal process of diazinon.

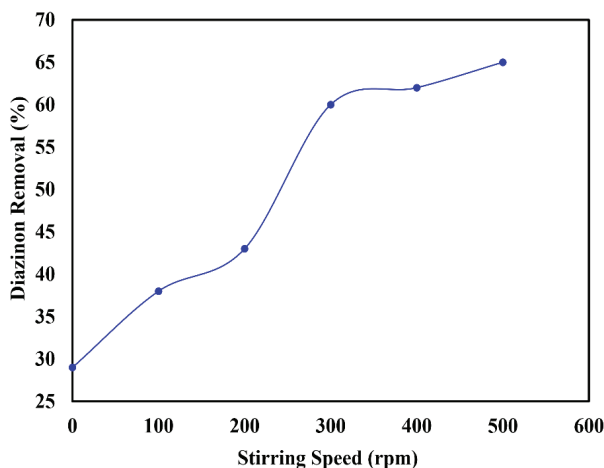


Fig. 9. Effect of stirring speed on removal efficiency of diazinon (diazinon concentration = 12 ppm, amount of adsorbent = 3 mg, contact time = 7 minutes, natural pH, and room temperature)

3.3. Adsorption isotherm

The adsorption isotherm can be used to study, estimation of the affinity between Cd MOF and diazinon, the adsorption mechanism and predict the maximum adsorption capacity of the Cd MOF. Here, three isotherm models (Temkin, Freundlich, and Langmuir isotherm) were applied. The Freundlich isotherm is applicable to the non-uniform adsorption processes of adsorbed molecules occurring on heterogeneous adsorbent surfaces. Multilayer adsorption is considered in this isotherm [37]. Temkin isotherm considers for accounting the effects of indirect adsorbate/adsorbate interactions on the adsorption process. It shows that there are various energetical sites on the adsorbent surface, in which adsorption of adsorbate occurs on the energetic sites at first. It is supposed that by increasing the surface coverage, the heat of absorption of the molecules in the layer decreases linearly. The Temkin isotherm model is reliable just for the intermediate range of dye

concentrations [38]. The Langmuir adsorption isotherm takes into describes the homogenous surface that a single surface site of adsorbent is occupied by a single adsorbate molecule. The Langmuir isotherm assumes that there is not any lateral interaction between the adsorbed molecules [39]. Langmuir, Temkin, and Freundlich isotherm represent according to the following Equations (3-5):

$$C_e / Q_e = 1/K_L Q_L + C_e/Q_L \quad \text{Langmuir isotherm} \quad (\text{Eq. 3})$$

$$Q_e = (RT/b_T) \ln K_T + (RT/b_T) \ln C_e \quad \text{Temkin isotherm} \quad (\text{Eq. 4})$$

$$\ln Q_e = \ln K_f + (1/n) \ln C_e \quad \text{Freundlich isotherm} \quad (\text{Eq. 5})$$

Where C_e (mg L^{-1}) is the equilibrium concentration of diazinon solution, Q_e (mg g^{-1}) is the amount of diazinon adsorbed by Cd MOF at equilibrium. R is gas constant ($8.314 \text{ J mol}^{-1}\text{K}^{-1}$) and T is temperature (K) that room temperature was taken into account. K_L and Q_L (the Langmuir monolayer adsorption capacity), b_T and K_T , K_f (adsorption capacity), and $1/n$ (adsorption intensity and adsorption capacity), are empirical constants parameters that affecting the adsorption process for Langmuir, Temkin, and Freundlich isotherms respectively [40].

As shown in Figure 10 the plots of Q_e vs. $\ln C_e$, $\ln Q_e$ vs. $\ln C_e$, and C_e/Q_e vs. C_e were used to calculate the constant parameters of Temkin, Freundlich, and Langmuir isotherms respectively. All parameters and correlation coefficient are listed in Table 1. The Langmuir isotherm gave the highest correlation coefficient, which was 0.98 at room temperature revealing that the adsorption of diazinon on the Cd MOF is perfectly described by this model.

3.4. Thermodynamic

The thermodynamic parameters of the

adsorption process were used to determine the spontaneity of the adsorption process at various temperatures. Change in enthalpy ΔH (kJ mol^{-1}), entropy ΔS ($\text{J mol}^{-1} \text{K}^{-1}$), and Gibbs free energy ΔG (kJ mol^{-1}) was calculated using the following equations 6 and 7:

$$\ln(Q_e/C_e) = \Delta S/R - \Delta H/RT \quad (\text{Eq. 6})$$

$$\Delta G = \Delta H - T\Delta S \quad (\text{Eq. 7})$$

ΔH and ΔS can be provided from the slope ($\Delta H/R$) and intercept ($\Delta S/R$) of the plot of $\ln(Q_e/C_e)$ vs. $1/T$ (Fig. 11). The calculated values of thermodynamic parameters are shown in table 2. The negative amount of ΔG indicates that the feasibility of the adsorption process and its spontaneous nature. The positive value of ΔH describes that the adsorption of diazinon by the Cd MOF is endothermic.

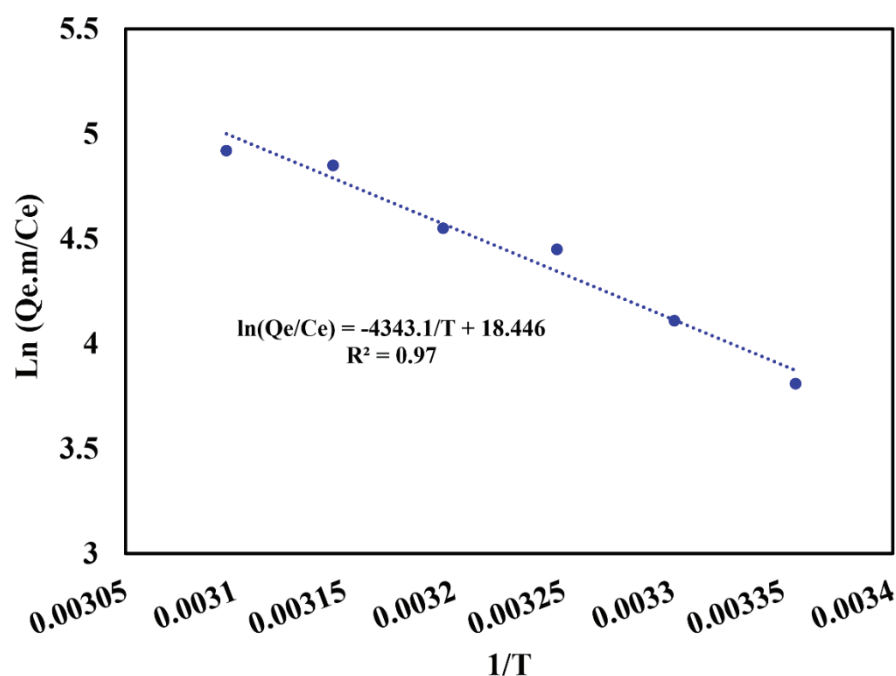


Fig. 11. Plot of $\ln(Q_e.m/C_e)$ vs. $1/T$ to give thermodynamic parameters

Table 2. Thermodynamic parameters for adsorption of diazinon on Cd MOF

Diazinon concentration (ppm)	ΔH (KJ mol^{-1})	ΔS ($\text{KJ mol}^{-1}\text{K}^{-1}$)	ΔG					
			(KJ mol^{-1})					
			298 K	303 K	308 K	313 K	318 K	323 K
12	36.11	0.15	-81.8	-82.6	-83.3	-84.1	-84.9	-85.6

3.5. Kinetic

Adsorption kinetics of diazinon removal were studied using Pseudo-first-order, pseudo-second-order and intraparticle diffusion models to identify the rapid initial phase of adsorption, chemisorptions and intra- particle diffusion. The linear forms of kinetic models are given as Equation 8-10:

$$\ln(Q_e - Q_t) = \ln Q_e - k_1 t \quad (\text{Pseudo first order kinetics})$$

(Eq. 8)

$$t/Q_t = t/Q_e + 1/k_2 Q_e^2 \quad (\text{Pseudo second-order kinetics})$$

(Eq. 9)

$$Q_t = k_i t^{1/2} + C \quad (\text{Intraparticle diffusion})$$

(Eq. 10)

Where, Q_t (mg g^{-1}) and Q_e (mg g^{-1}) refer to the amount of diazinon adsorbed at time t (min) and equilibrium respectively. k_1 (min^{-1}), k_2 ($\text{g mg}^{-1}\text{min}^{-1}$), and k_i ($\text{mg g}^{-1}\text{min}^{1/2}$) are rate constant of adsorption for pseudo-first order, pseudo second order and intraparticle diffusion respectively. In intraparticle diffusion, constant C reflects the boundary layer effect [39].

Table 3 shows a list of kinetic parameters for various initial concentrations of diazinon. Compared to the pseudo-first-order and intraparticle diffusion, the pseudo-second-order model showed a higher regression coefficient and was selected as the model for the absorption kinetics of diazinon removal.

4. Conclusion

In this work, Cd based metal organic frameworks (Cd MOFs) were synthesized by a simple and cost-effective hydrothermal route using fumaric acid as a linker. The prepared Cd MOF used for removal of diazinon from water. The absorbent dose, pH, temperature, diazinon concentration, contact time and stirring speed were optimized as affecting parameters and the best condition was reported in this paper. Various isotherm and kinetic models were investigated for the removal of diazinon using the prepared Cd MOF and the Langmuir isotherm and pseudo-second -order kinetic model was suggested for uptake of diazinon on the Cd MOFs through an endothermic process. According to results, Cd MOF can act as an effective adsorbent for removal the pesticides from water through a fast, cost-effective and simple route.

Table 3. Kinetic parameters for adsorption of diazinon on Cd MOF

Qi (mg g^{-1})	Qe (mg g^{-1})	Pseudo First order			Pseudo Second order			Intraparticle		
		Qe	K1	R ²	Qe	K2	R ²	C	Ki	R ²
4	29.88	1.24	0.58	0.98	43.01	0.032	0.99	6.59	10.44	0.86
6	54.9	1.18	0.18	0.7	46.51	0.027	0.98	10.59	14.45	0.72
8	63.9	1.31	0.21	0.74	58.14	0.018	0.98	10.37	18.67	0.76
10	69.12	1.34	0.19	0.82	60.24	0.019	0.99	11.91	18.9	0.82
12	72	1.35	0.18	0.81	60.24	0.02	0.99	13.35	18.48	0.84

5. References:

- [1] M. Abdollahi, S. Mostafalou, S. Pournourmohammadi, S. Shadnia, Oxidative stress and cholinesterase inhibition in saliva and plasma of rats following subchronic exposure to malathion, *Comparative Biochemistry and Physiology Part C: Toxicol. Pharmacol.*, 137 (2004) 29-34. <https://doi.org/10.1016/j.cca.2003.11.002>
- [2] M.D. Shah, M. Iqbal, Diazinon-induced oxidative stress and renal dysfunction in rats, *Food Chem. Toxicol.*, 48 (2010) 3345-3353. <https://doi.org/10.1016/j.fct.2010.09.003>
- [3] E. Noroozian, Solid phase microextraction of organochlorine pesticides in water using MWCNTs-doped polypyrrole coated on steel fiber, *Anal. Methods Environ. Chem. J.*, 3 (2020) 40-51. <https://doi.org/10.24200/amecj.v3.i04.117>
- [4] R. Kamanyire, L. Karalliedde, Organophosphate toxicity and occupational exposure, *Occup. Med.*, 54 (2004) 69-75. <https://doi.org/10.1093/occmed/kqh018>
- [5] I.B. Obinna, E.C. Ebere, A review: Water pollution by heavy metal and organic pollutants: Brief review of sources, effects and progress on remediation with aquatic plants, *Anal. Methods Environ. Chem. J.*, 2 (2019) 5-38. <https://doi.org/10.24200/amecj.v2.i03.66>
- [6] S. Selmi, S. El-Fazaa, N. Gharbi, Oxidative stress and cholinesterase inhibition in plasma, erythrocyte and brain of rats' pups following lactational exposure to malathion, *Environ. Toxicol. Pharmacol.*, 34 (2012) 753-760. <https://doi.org/10.1016/j.etap.2012.09.012>
- [7] M.E. Buyukokuroglu, M. Cemek, Y. Yurumez, Y. Yavuz, A. Aslan, Antioxidative role of melatonin in organophosphate toxicity in rats, *Cell Biol. Toxicol.*, 24 (2008) 151-158. <https://doi.org/10.1007/s10565-007-9024-z>
- [8] M.E. Büyükokuroğlu, M. Cemek, M. Tosun, Y. Yürümez, O. Baş, Y. Yavuz, Dantrolene may prevent organophosphate-induced oxidative stress and muscle injury, *Pesticide Biochem. Physiol.*, 92 (2008) 156-163. <https://doi.org/10.1016/j.pestbp.2008.07.012>
- [9] A. Mitra, M. Sarkar, C. Chatterjee, Modulation of immune response by organophosphate pesticides: Mammals as potential model, *Proceedings of the Zoological Society*, Springer, 2019, pp. 13-24. <https://doi.org/10.1007/s12595-017-0256-5>
- [10] M.K. Mahani, A.R. Khanchi, M. Heidari, A. Ahmadi, A novel inductively coupled plasma atomic emission spectrometry method for uranium isotope ratio measurements using chemometric techniques, *J. Anal. Atom. Spect.*, 25 (2010) 1659-1660. <https://doi.org/10.1039/C004761A>
- [11] P. Sharma, A. Sharma, N.D. Jasuja, S.C. Joshi, Organophosphorous compounds and oxidative stress: a review, *Toxicol. Environ. Chem.*, 96 (2014) 681-698. <https://doi.org/10.1080/02772248.2014.972045>
- [12] M. Kushwaha, S. Verma, S. Chatterjee, Profenofos, An acetylcholinesterase-inhibiting organophosphorus pesticide: a short review of its usage, Toxicity, and Biodegradation, *J. Environ. Quality*, 45 (2016) 1478-1489. <https://doi.org/10.2134/jeq2016.03.0100>
- [13] S. Karami-Mohajeri, M. Abdollahi, Toxic influence of organophosphate, carbamate, and organochlorine pesticides on cellular metabolism of lipids, proteins, and carbohydrates: a systematic review, *Human Exp. Toxicol.*, 30 (2011) 1119-1140. <https://doi.org/10.1177/0960327110388959>
- [14] M.K. Mahani, M.G. Maragheh, Simultaneous determination of sodium, potassium, manganese and bromine in tea by standard addition neutron activation analysis, *Food Anal. Methods*, 4 (2011) 73-76. <https://doi.org/10.1007/s12161-009-9120-1>
- [15] H. Sepehrian, S. Waqif-Husain, J. Fasihi, M.K. Mahani, Adsorption behavior of molybdenum on modified mesoporous zirconium silicates, *Sep. Sci. Technol.*, 45 (2010) 421-426. <https://doi.org/10.1080/01496390903423519>

- [16] E. Zolfonoun, Solid phase extraction and determination of indium using multiwalled carbon nanotubes modified with magnetic nanoparticles, *Anal. Methods Environ. Chem. J.*, 1 (2018) 5-10. <https://doi.org/10.24200/amecj.v1.i01.14>
- [17] A. Zarei, M. Arjomandi, Synthesis and performance of graphene and activated carbon composite for absorption of three-valance arsenic from wastewater, *Anal. Methods Environ. Chem. J.*, 2 (2019) 63-72. <https://doi.org/10.24200/amecj.v2.i01.53>
- [18] C. Jamshidzadeh, H. Shirkhanloo, A new analytical method based on bismuth oxide-fullerene nanoparticles and photocatalytic oxidation technique for toluene removal from workplace air, *Anal. Methods Environ. Chem. J.*, 2 (2019) 73-86. <https://doi.org/10.24200/amecj.v2.i01.55>
- [19] M. Gou, B.B. Yarahmadi, Separation and determination of lead in human urine and water samples based on thiol functionalized mesoporous silica nanoparticles packed on cartridges by micro column fast micro solid-phase extraction, *Anal. Methods Environ. Chem. J.*, 2 (2019) 39-50. <https://doi.org/10.24200/amecj.v2.i03.72>
- [20] S. Fakhraie, A. Ebrahimi, Facile synthesis of a modified HF-free MIL-101 (Cr) nanoadsorbent for extraction nickel in water and wastewater samples, *Anal. Methods Environ. Chem. J.*, 3 (2020) 59-73. <https://doi.org/10.24200/amecj.v3.i02.103>
- [21] M.H. Mokari-Manshadi, M. Mahani, Z. Hassani, D. Afzali, E. Esmailzadeh, Synthesis of Mesoporous Molybdenum Disulfide (MoS₂): A Photocatalyst for Removal of Methylene Blue, *J. Nanosci. Nanotechnol.*, 17 (2017) 8864-8868. <https://doi.org/10.1166/jnn.2017.14317>
- [22] F. Khakbaz, M. Mirzaei, M. Mahani, Enhanced adsorption of crystal violet using Bi³⁺-intercalated Cd-MOF: isotherm, kinetic and thermodynamic study, *Particulate Sci. Technol.*, (2022) 1-13. <https://doi.org/10.1080/02726351.2022.2032890>
- [23] J. Cao, X. Li, H. Tian, Metal-organic framework (MOF)-based drug delivery, *Curr. Med. Chem.*, 27 (2020) 5949-5969. <https://doi.org/10.2174/0929867326666190618152518>
- [24] V. Stavila, R. Parthasarathi, R.W. Davis, F. El Gabaly, K.L. Sale, B.A. Simmons, S. Singh, M.D. Allendorf, MOF-based catalysts for selective hydrogenolysis of carbon-oxygen ether bonds, *ACS Catal.*, 6 (2016) 55-59. <https://doi.org/10.1021/acscatal.5b02061>
- [25] S. Roy, S. Halder, M.G. Drew, P.P. Ray, S. Chattopadhyay, Fabrication of an active electronic device using a hetero-bimetallic coordination polymer, *ACS Omega*, 3 (2018) 12788-12796. <https://doi.org/10.1021/acsomega.8b02025>
- [26] V.O.N. Njoku, C. Arinze, I.F. Chizoruo, E.N. Blessing, A Review: Effects of air, water and land dumpsite on human health and analytical methods for determination of pollutants, *Anal. Methods Environ. Chem. J.*, 4 (2021) 80-106. <https://doi.org/10.24200/amecj.v4.i03.147>
- [27] M.G. Campbell, M. Dincă, Metal-organic frameworks as active materials in electronic sensor devices, *Sensors*, 17 (2017) 1108. <https://doi.org/10.3390/s17051108>
- [28] Z.-H. Zhang, L. Xu, H. Jiao, Ionothermal synthesis, structures, properties of cobalt-1, 4-benzenedicarboxylate metal-organic frameworks, *J. Solid State Chem.*, 238 (2016) 217-222. <https://doi.org/10.1016/j.jssc.2016.03.028>
- [29] S.J. Yang, T. Kim, K. Lee, Y.S. Kim, J. Yoon, C.R. Park, Solvent evaporation mediated preparation of hierarchically porous metal organic framework-derived carbon with controllable and accessible large-scale porosity, *Carbon*, 71 (2014) 294-302. <https://doi.org/10.1016/j.carbon.2014.01.056>
- [30] N.M. Kazemi, A novel sorbent based on metal-organic framework for mercury separation from human serum samples by ultrasound assisted-ionic liquid-solid phase

- microextraction, *Anal. Methods Environ. Chem. J.*, 2 (2019) 67-78. <https://doi.org/10.24200/amecj.v2.i03.68>
- [31] L.S. Germann, A.D. Katsenis, I. Huskić, P.A. Julien, K. Uzarevic, M. Etter, O.K. Farha, T. Friscic, R.E. Dinnebier, Real-time in situ monitoring of particle and structure evolution in the mechanochemical synthesis of UiO-66 metal–organic frameworks, *Cryst. Growth Des.*, 20 (2019) 49-54. <https://doi.org/10.1021/acs.cgd.9b01477>
- [32] A.M. Antonio, J. Rosenthal, E.D. Bloch, Electrochemically Mediated Syntheses of Titanium (III)-Based Metal–Organic Frameworks, *J. Am. Chem. Soc.*, 141 (2019) 11383-11387. <https://doi.org/10.1021/jacs.9b05035>
- [33] N. Motakef-kazemi, Zinc based metal–organic framework for nickel adsorption in water and wastewater samples by ultrasound assisted-dispersive-micro solid phase extraction coupled to electrothermal atomic absorption spectrometry, *Anal. Methods Environ. Chem. J.*, 3 (2020) 5-16. <https://doi.org/10.24200/amecj.v3.i04.123>
- [34] M. Taddei, D.A. Steitz, J.A. van Bokhoven, M. Ranocchiari, Continuous-Flow Microwave Synthesis of Metal–Organic Frameworks: A Highly Efficient Method for Large-Scale Production, *Chem. A Euro. J.*, 22 (2016) 3245-3249. <https://doi.org/10.1002/chem.201505139>
- [35] C. McKinsty, R.J. Cathcart, E.J. Cussen, A.J. Fletcher, S.V. Patwardhan, J. Sefcik, Scalable continuous solvothermal synthesis of metal organic framework (MOF-5) crystals, *Chem. Eng. J.*, 285 (2016) 718-725. <https://doi.org/10.1016/j.cej.2015.10.023>
- [36] F. Pourbahman, A. Monzavi, Z. Khodadadi, S.S. Homami, Reusable and sustainable graphene oxide/metal–organic framework-74/Fe₃O₄/polytyramine nanocomposite for simultaneous trace level quantification of five fluoroquinolones in egg samples by high performance liquid chromatography, *Anal. Methods Environ. Chem. J.*, 4 (2021) 5-24. <https://doi.org/10.24200/amecj.v4.i02.135>
- [37] N. Ayawei, A.N. Ebelegi, D. Wankasi, Modelling and interpretation of adsorption isotherms, *J. Chem.*, 2017 (2017). <https://doi.org/10.1155/2017/3039817>
- [38] H. Shahbeig, N. Bagheri, S.A. Ghorbanian, A. Hallajisani, S. Poorkarimi, A new adsorption isotherm model of aqueous solutions on granular activated carbon, *World J. Model. Simul.*, 9 (2013) 243-254. <http://doi.org/10.1.1.571.6718>
- [39] B. Kaith, J. Sharma, Sukriti, S. Sethi, T. Kaur, U. Shanker, V. Jassal, Fabrication of green device for efficient capture of toxic methylene blue from industrial effluent based on K₂Zn₃[Fe(CN)₆]₂·9H₂O nanoparticles reinforced gum xanthan-psyllium hydrogel nanocomposite, *J. Chin. Adv. Mater. Soc.*, 4 (2016) 249-268. <https://doi.org/10.1080/22243682.2016.1214923>
- [40] A. Mohammadi, A. Alinejad, B. Kamarehie, S. Javan, A. Ghaderpoury, M. Ahmadpour, M. Ghaderpoori, Metal-organic framework UiO-66 for adsorption of methylene blue dye from aqueous solutions, *Int. J. Environ. Sci. Technol.*, 14 (2017) 1959-1968. <https://doi.org/10.1016/j.cca.2003.11.002>